Commentary

The inner inner core of Earth

Don L. Anderson*

Seismological Laboratory, California Institute of Technology, Pasadena, CA 91125

The solid inner core (Fig. 1) is the most remote and enigmatic part of our planet, and, next to the crust, is the smallest "official" subdivision of Earth's interior. It was discovered in 1936 (1), and by 1972 it was established that it was solid, albeit with a very small rigidity (2–4). By 1993 it had been established that it was crystalline (5). The inner core is isolated from the rest of Earth by the low-viscosity fluid outer core, and it can rotate, nod, wobble, precess, oscillate, and even flip over, being only loosely constrained by the surrounding shells. Its existence, size, and properties constrain the temperature and mineralogy near the center of the Earth. Among its anomalous characteristics are low rigidity and viscosity (compared with other solids), bulk attenuation, extreme anisotropy, and superrotation (or deformation; refs. 5–8). From seismic velocities and cosmic abundances, we know that it is composed mainly of iron-nickel crystals, and the crystals must exhibit a large degree of common orientation. The inner core is predicted to have very high thermal and electrical conductivity, a nonspherical shape, and frequency-dependent properties; also, it may be partially molten. It may be essential for the existence of the magnetic field and for polarity reversals of this field (D. Gubbin, D. Alfe, G. Masters, D. Price, and M. Gillan, unpublished work). Freezing of the inner core and expulsion of impurities is likely responsible for powering the geodynamo. Yet, the inner core represents less than 1% of the volume of Earth, and only a few seismic waves ever reach it and return to the surface. The inner core is a small target for seismologists, and seismic waves are distorted by passing through the entire Earth before reaching it. Conditions near the center of the Earth are so extreme that both theoreticians and experimenters have difficulty in duplicating its environment. Nevertheless, there has been a recent flurry of activity about the inner core by seismologists, geochemists, dynamicists, materials scientists, and geodynamo theoreticians. Almost everything known or inferred about the inner core from seismology or from indirect inference is controversial. In this issue of PNAS, Ishii and Dziewoński (8) add further intrigue and complication to phenomena near the center of the Earth, and they suggest a complex history for this small object.

Almost everything known or inferred about the inner core, from seismology or indirect inference, is controversial.

Planets differentiate as they accrete and gain gravitational energy. Timing of this differentiation is a long-standing goal of Earth science (9–13). Density stratification explains the locations of the crust, mantle, and core. The inner core is likely also the result of chemical stratification, although the effect of pressure on the melting point would generate a solid inner core even if it were chemically identical to the outer core. Low-density materials are excluded when solidification is slow, so the inner core may be purer and denser than the outer core. As the inner core crystallizes and the outer core cools, the material held in solution and suspension will plate out, or settle, at the core mantle boundary and may be incorporated into the lowermost mantle. The mantle is usually treated as a chemically homogeneous layer, but this is unlikely. Denser silicates, possibly silicon- and iron-rich, also gravitate toward the lower parts of the mantle. Crustal and shallow mantle materials were sweated out of the Earth as it accreted, and some were apparently never in equilibrium with core material. The effect of pressure on physical properties implies that the mantle and core probably stratified irreversibly upon accretion, that only the outer shells of the mantle participate in surface processes such as volcanism and plate tectonics, and that only the deeper layers currently interact with the core.

The crust, upper mantle, lower mantle, core, and inner core are the textbook subdivisions of the Earth's interior. Seismic tomography is used to map large-scale lateral variations in these major subdivisions. Higher resolution seismic techniques have been used to discover and map small-scale features at the top and bottom of the core (14–16). The classical boundaries inside the Earth (6) were all discovered in the early part of the last century. In the 1960s, boundaries internal to the mantle were discovered at depths of 400 and 650 km and were attributed to solid–solid phase changes (17), in contrast to the others which are chemical or solidification boundaries. More recently, a probable chemical discontinuity was found deep in the mantle (16), and another one was inferred near 900 km (18). Seismic discontinuities are conventionally found by the reflection and refraction of seismic waves, but recently factors such as anisotropy, attenuation, scattering, spectral density, and statistical decorrelations have been used to find the more subtle features. The new region deep in the inner core represents a change in character of the anisotropy pattern (8) and may represent a fundamentally different phenomenon.

The long-standing controversy regarding a drawn-out (100 million years) vs. a rapid ($\approx$1 million year) terrestrial accretion seems to be resolving itself in favor of the shorter time scales and a high-temperature origin. Geophysical data require rapid accretion of Earth and early formation of the core (9). Until recently, rapid accretion has been at odds with accretional theory and isotopic data, but now, these disciplines are also favoring a contracted time scale. A variety of isotopes have confirmed short time intervals between the formation of the solar system and planetary differentiation processes (10–13). This finding has bearing on the age of the inner core and its cooling history.

There are three quite different mechanisms for making a planetary core. In the homogeneous accretion hypothesis, the silicates and the metals accrete together but, as the Earth heats up, the heavy metals percolate downwards, eventually forming large dense accumulations that sink rapidly toward the center, taking the siderophile elements with them. In the heterogenous accretion hypothesis, the refractory condensates (including iron and nickel) from a cooling nebula start to form

See companion article on page 14026.

*E-mail: dla@gps.caltech.edu.

www.pnas.org/cgi/doi/10.1073/pnas.232565899

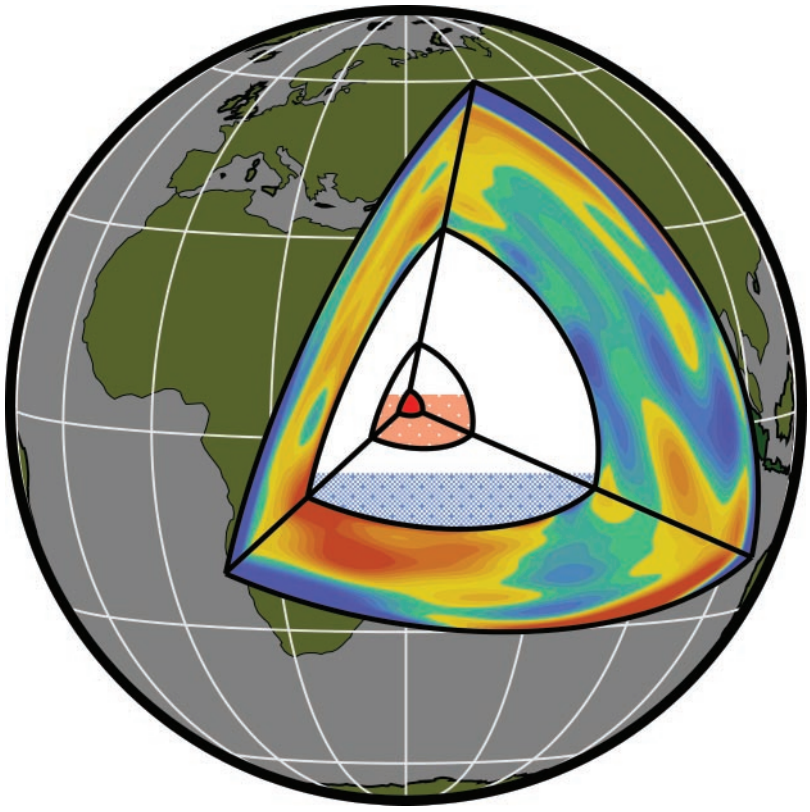

Fig. 1. View of the Earth's interior. The volumetric relation of the various regions of the core to the whole Earth is shown: outer core (pale blue) occupies 15%, the inner core (pink) occupies less than 1%, and the innermost inner core (red) constitutes only 0.01% of the Earth's volume. The Earth's core lies beneath 3,000-km thick, heterogeneous mantle (anomalies with higher than average seismic speed are shown in blue and those with lower than average speed are shown in red), making investigations of core properties challenging.

the nucleus of a planet before the bulk of the silicates and volatiles are available. The late veneer contributes low-temperature condensates and gases, including water, from the far reaches of the solar system. Finally, large late impacts can efficiently and rapidly inject their metallic cores to the center of the impacted planet and trigger additional separation of iron from the mantle. The Moon is a byproduct of one of these late impacts. The material in the core may, therefore, have multiple origins and a complex history. Other issues regarding the inner core involve its age, growth rate, density, temperature, texture, and internal energy sources (refs. 8 and 19–21, and D. Gubbin, D. Alfe, G. Masters, D. Price, and M. Gillan, unpublished work).

The outer core is usually considered to be completely molten because of its low viscosity and inability to transmit shear waves. However, it could contain more than 50% suspended crystals and still behave as a fluid. The boundary of the inner core then could represent the crossing of the geotherm with the melting curve (the conventional explanation) or a compaction boundary where the particle density of the slurry exceeds a threshold. It is usually assumed that the outer core is homogeneous, entirely fluid, and convects turbulently. The inner core also may contain a substantial melt fraction, particularly if there is a large interval between the solidus and the liquidus. It has also been proposed that the inner core is a viscous fluid or a metallic glass (19). The new results on anisotropy make this unlikely. The low, inferred viscosity of the inner core means that it can deform and convect from the influence of tidal and rotational stresses and outer core motions as well as from internally generated stresses. The inner core is one of the few places in the interior where one might expect to see changes on a human timescale. It may exhibit semirigid differential rotation with respect to the mantle but also, and more likely, nonrigid or plastic deformation. Anisotropy is one indicator of such deformation or convection.

Crystals are anisotropic and tend to be oriented by sedimentation, freezing, recrystallization, deformation, and flow. Therefore, we expect the solid portions of the Earth to be anisotropic to the propagation of seismic waves and other material properties. Despite these expectations, seismology proceeded and flourished with the assumption of isotropy until the 1960s. At this point, the theory of seismic anisotropy was worked out and observations verified the expectations (see references in ref. 6). Nevertheless, most seismologists ignored anisotropy until fairly recently in the progress of seismology. Not only is anisotropy a useful tool for determining composition, mineralogy, and deformation from seismology, but Earth models based on isotropy can be completely wrong. Anisotropy is not simply a small perturbation to an essentially isotropic Earth. The variation of seismic wave speeds as a function of direction can be greater than those caused by temperature and composition. In the case of the inner inner core (8), the penetrating seismic waves travel almost radially, so very little information is extractable, except the variation of travel time with azimuth, e.g., equatorial vs. polar paths, or with waves propagating in different directions in the equatorial plane. The size of the Fresnel zone also limits the seismic resolution of the innermost core. Fortunately, high-pressure iron crystals have a large anisotropy (21, 22); otherwise, little could be said about heterogeneity or rotation/deformation of the inner core.

The shape and fabric of the inner core are affected by gravitational forces from the mantle, electromagnetic and viscous stresses from the outer core, and rotational and tidal stresses. These stresses cause irreversible plastic flow, crystal alignment, and recrystallization. Seismic anisotropy is one result.

The inner core is subjected to a variety of external stresses involving variations in orbital and rotational parameters, tides, gravitational tugs from the mantle, viscous drag of the outer core, and electromagnetic forces. It also may generate internal stresses by thermal and chemical variations, anisotropy and cooling, and respond to these by porous flow, differential rotation, convection, and deformation and creation of material anisotropy. Anisotropy can also form by freezing of the inner core and sedimentation on its surface. Small-scale heterogeneity, for example, can melt channels or exsolution fabric and can also generate apparent anisotropy.

The conventional explanation of the formation of the solid inner core involves slow cooling and crystallization. Because the melting temperature increases with pressure, the core will solidify from the center outwards. But this effect also means that as pressure increases because of accretion, the core can pressure-freeze when the Earth reaches a critical size, unless there is a large amount of superheat. Although we know that the magnetic field is ancient and that a solid and growing inner core may be essential to its

existence, it is possible that catastrophic events such as the Moon-forming impact may have caused the inner core to reform one or more times. Initial superheat and episodic growth will possibly resolve some of the current energy problems (ref. 20, and D. Gubbin, D. Alfe, G. Masters, D. Price, and M. Gillan, unpublished work). A growing inner core is needed to power the current dynamo, but rapid cooling may have powered the ancient dynamo (D. Gubbin, D. Alfe, G. Masters, D. Price, and M. Gillan, unpublished work). The inner core may, therefore, be much younger than the Earth. The heterogeneity and anisotropy of the inner core may help constrain its apparently complex history.

The inner core has bearing on a wide variety of geophysical, geochemical (23), magnetic field, and planetary problems. Anisotropy is not only an important parameter bearing on core dynamics, but it also makes it possible to characterize and monitor the inner core. Anisotropy has become an indispensable tool to seismologists, rather than the bother it was once considered. And the prospect of finding differences the next time we look offers an excitement unusual in most routine mapping endeavors.

1. Lehmann, I. (1936) *Bur. Centr. Seism. Inst. A* **14,** 3–31.
2. Derr, J. (1969) *J. Geophys. Res.* **74,** 5202–5220.
3. Julian, B., Davies, D. & Sheppard, R. (1972) *Nature* **235,** 317–318.
4. Anderson, D. L., Sammis, C. G. & Jordan, T. H. (1971) *Science* **171,** 1103–1112.
5. Tromp, J. (1993) *Nature* **366,** 678–681.
6. Anderson, D. L. (1989) *Theory of the Earth* (Blackwell Scientific, Oxford), p. 366.
7. Song, X. & Richards, P. (1996) *Nature* **382,** 221–224.
8. Ishii, M. & Dziewoński, A. M. (2002) *Proc. Natl. Acad. Sci. USA* **99,** 14026–14030.
9. Anderson, D. L. & Hanks, T. C. (1972) *Nature* **5355,** 387–388.
10. Cameron, A. (2002) *Nature* **418,** 924–925.
11. Klein, T., Munker, C., Mezger, K. & Palme, H. (2002) *Nature*, **418,** 952–955.
12. Schonbachler, M., Rehkämper, M., Halliday, A., Lee, D.-C., Bourot-Denise, M., Zanda, B., Hattendorf, B. & Günther, D. (2002) *Science* **295,** 1705–1708.
13. Yin, Q. (2002) *Nature* **418,** 949–952.
14. Song, X. & Helmberger, D. V. (1998) *Science* **282,** 924–927.
15. Wen, L. & Helmberger, D. V. (1998) *Science* **279,** 1701–1703.
16. Lay, T. & Helmberger, D. V. (1983) *Geophys. J. R. Astron. Soc.* **75,** 799–838.
17. Anderson, D. L. (1967) *Science* **157,** 1165–1173.
18. Wen, L. & Anderson, D. L. (1997) *Earth Planet. Sci. Lett.* **146,** 367–377.
19. Bazhkin, V. V. (1998) *JETP Lett.* **68,** 502–508.
20. Steinle-Neumann, G., Stixrude, L., Cohen R. & Gülseren, O. (2001) *Nature* **413,** 57–60.
21. Jephcoat, A. & Refson, K. (2001) *Nature* **413,** 27–30.
22. Jeanloz, R. & Wenk, H. (1988) *Geophys. Res. Lett.* **15,** 72–75.
23. Meibom, A. & Frei, R. (2002) *Science* **296,** 516–518.

Corrections

BIOCHEMISTRY. For the article "Interaction of RNA polymerase with forked DNA: Evidence for two kinetically significant intermediates on the pathway to the final complex," by Laura Tsujikawa, Oleg V. Tsodikov, and Pieter L. deHaseth, which appeared in number 6, March 19, 2002, of *Proc. Natl. Acad. Sci. USA* (**99,** 3493–3498; First Published March 12, 2002; 10.1073/pnas.062487299), the authors note the following concerning RNA polymerase (RNAP) concentrations. No correction was made for the fraction of RNAP (0.5) that is active in promoter binding. With this correction, the values of K_1 and K_{app} (but not K_f) would increase by about a factor of 2. The relative values would remain essentially unchanged. Also, the legends to Figs. 2, 3, and 5 contain errors pertaining to the symbols used for data obtained with and without heparin challenge, the duration of the challenge, and the concentration of added heparin. The figures and the corrected legends appear below.

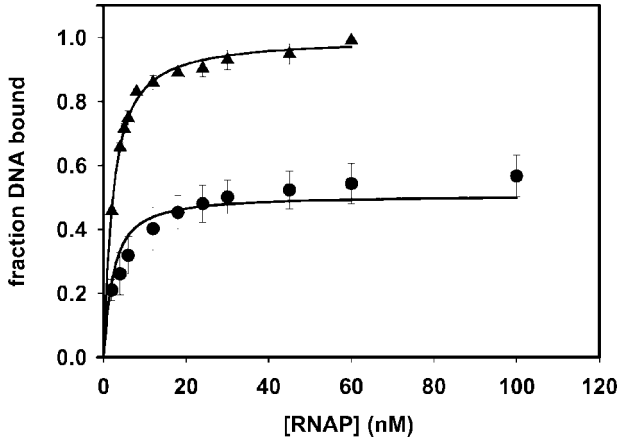

Fig. 2. Determination of equilibrium affinities by titration of wt Fork with RNAP. The reactions contained 1 nM wt Fork and variable amounts of RNAP as shown and were analyzed by electrophoretic mobility shift immediately (▲; data shown are averages of three independent experiments) or after a challenge with 100 μg/ml heparin for 10 min (●; data shown are averages of four independent experiments). The curves shown reflect the simultaneous error-weighted fits of the data to Eqs. **3** and **4–7**. The parameters are shown in Table 1 (line 1).

www.pnas.org/cgi/doi/10.1073/pnas.013667699

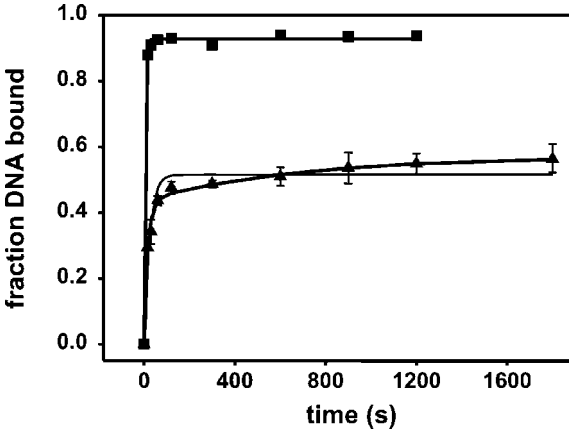

Fig. 3. Kinetics of complex formation. RNAP (65 nM) and wt forked DNA (1 nM) were incubated for various time intervals and then complex formation was determined immediately (−heparin) or after a 2-min challenge with 100 μg/ml heparin (+heparin). The −heparin data (■) were fit (error-weighted) with Eq. **8** with $a_2 = 0$ ($k_{a-} = 0.10 \pm 0.01\ s^{-1}$) and the +heparin data (▲) with both single ($k_{a+} = 0.036 \pm 0.004\ s^{-1}$; thin line) and double-exponential ($k_{a_1} = 0.044 \pm 0.002\ s^{-1}$, $k_{a_2} = (5 \pm 3) \times 10^{-4}\ s^{-1}$; thick line) equations.

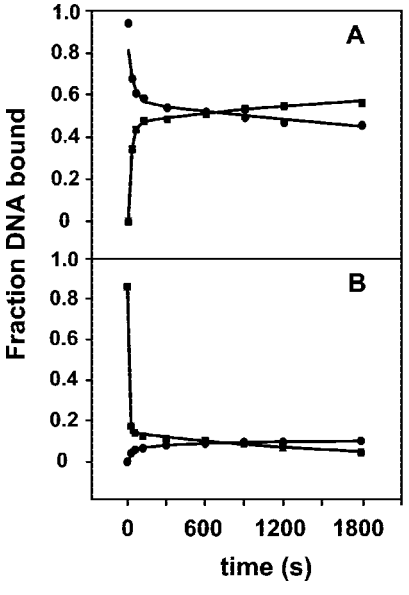

Fig. 5. Comparison of the kinetics for formation and dissociation of competitor-resistant complexes between RNAP and wt Fork. Association data were obtained as described in the text and the legend for Fig. 3 except the concentration of forked DNA was 10 nM. Dissociation kinetics were obtained by challenging with 100 μg/ml heparin a mixture of RNAP and forked DNA that had been incubated for 30 min. The curves represent double-exponential fits of the data to Eq. **10**. (*A*) wt RNAP. The observed association rate constants (■) are shown in the legend for Fig. 3; for the slow phase of the dissociation of the wt Fork–wt RNAP complex (●), $k_{d_2} = (1.3 \pm 0.2) \times 10^{-4}\ s^{-1}$. (*B*) YYW RNAP. The slow phase of the association reaction (●) has a $k_{a_2} = (1.1 \pm 0.3) \times 10^{-3}\ s^{-1}$; the slow phase of the dissociation reaction (■), a $k_{d_2} = (6 \pm 1) \times 10^{-4}\ s^{-1}$.

CORRECTIONS

CELL BIOLOGY. For the article "Nrdp1/FLRF is a ubiquitin ligase promoting ubiquitination and degradation of the epidermal growth factor receptor family member, ErbB3," by Xiao-Bo Qiu and Alfred L. Goldberg, which appeared in number 23, November 12, 2002, of *Proc. Natl. Acad. Sci. USA* (**99,** 14843–14848; First Published October 31, 2002; 10.1073/pnas.232580999), Fig. 4 should have appeared in color. In addition, the marker for the Ub band of Fig. 6*A* should be 14. The corrected figures and their legends appear below.

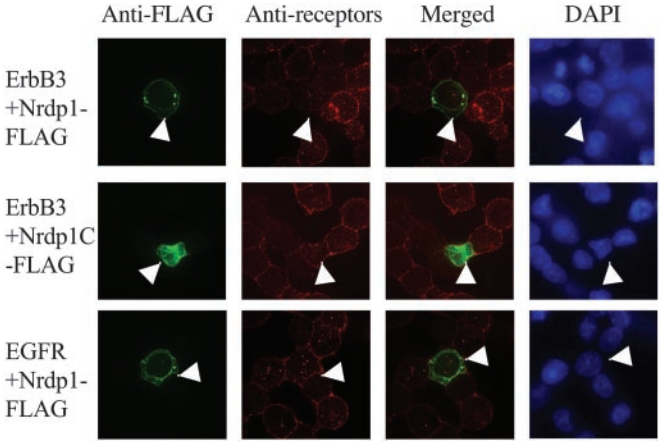

Fig. 4. Nrdp1 reduces levels of endogenous ErbB3. MDA-MB-468 cells were transfected with FLAG-tagged Nrdp1 or Nrdp1C. Localization of Nrdp1, Nrdp1C, ErbB3, or EGFR was visualized by confocal fluorescence microscopy after incubation with appropriate primary antibodies and FITC or Cy3 conjugates of secondary antibodies. Different images on each row, which are representative of many (>30) microscopic fields, are the same cells with different kinds of staining. The cells transfected with Nrdp1 or Nrdp1C are indicated by arrowheads. The nuclei of cells were visualized under UV light after staining with 4′,6-diamidino-2-phenylindole.

www.pnas.org/cgi/doi/10.1073/pnas.013671499

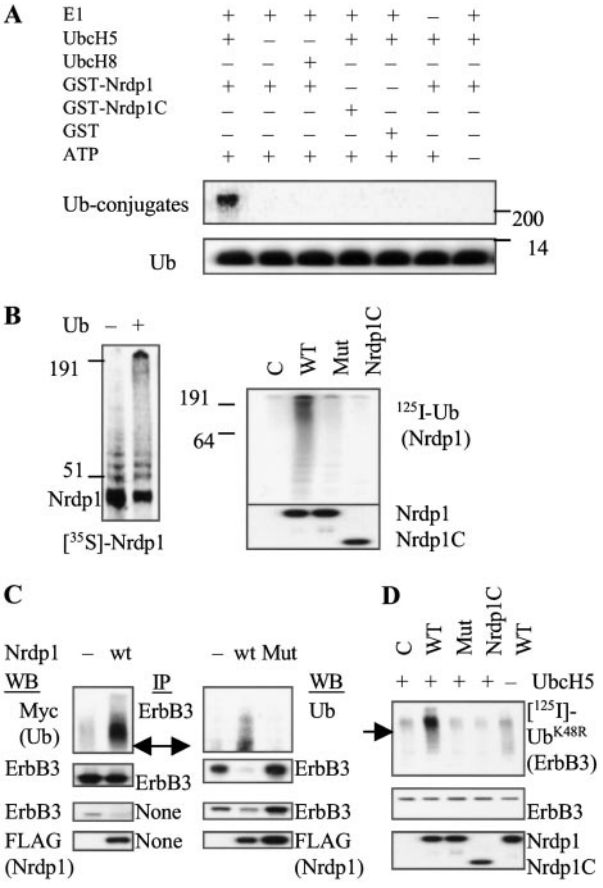

Fig. 6. Nrdp1 is a ubiquitin ligase promoting ubiquitination of itself and ErbB3. (*A*) Nrdp1-catalyzed formation of [^{125}I]ubiquitin conjugates was assayed *in vitro*. All of the components were expressed and purified from bacteria. (*B*) Autoubiquitination of Nrdp1 requires its RING finger domain. Wild-type, mutant (C34S/H36Q), and truncated Nrdp1 were immunopurified from the 293T cells transfected with their FLAG-tagged form and were used for *in vitro* ubiquitination assay. (*Left*) Nrdp1 was labeled *in vivo* with ^{35}S. (*Right*) Ubiquitin was labeled with ^{125}I. (*C*) Nrdp1 stimulates ErbB3 ubiquitination *in vivo*. The 293T cells were transfected with ErbB3, or cotransfected with ErbB3 and the wild-type or mutant (C34S/H36Q) Nrdp1-FLAG in the presence (*Left*) or the absence (*Right*) of pCMV-myc-Ub (kindly provided by Ron Kopito, Stanford University, Stanford, CA). ErbB3 ubiquitination was detected by Western blotting by using either anti-myc antibodies (Oncogene Research Products) or anti-Ub antibodies (Zymed) after immunoprecipitation by anti-ErbB3 antibodies. Arrows indicate 191-kDa markers. (*D*) Nrdp1 ubiquitinates endogenous ErbB3 *in vitro*. ErbB3 immunoprecipitated from the MDA-MB-453 cells was incubated with the lysates of 293T cells untransfected or transfected with wild-type, mutant (C34S/H36Q), or truncated Nrdp1-FLAG in the presence of [^{125}I]ubiquitin (K48R mutant). The ^{125}I-labeled ErbB3-ubiquitin conjugates on beads were separated on SDS/PAGE and analyzed by PhosphorImager after ubiquitination assays and precipitation from the reaction mix. Arrow indicates the 191-kDa marker.

GENETICS. For the article "Genetic and physiological data implicating the new human gene G72 and the gene for D-amino acid oxidase in schizophrenia," by Ilya Chumakov, Marta Blumenfeld, Oxana Guerassimenko, Laurent Cavarec, Marta Palicio, Hadi Abderrahim, Lydie Bougueleret, Caroline Barry, Hiroaki Tanaka, Philippe La Rosa, Anne Puech, Nadia Tahri, Annick Cohen-Akenine, Sylvain Delabrosse, Sébastien Lissarrague, Françoise-Pascaline Picard, Karelle Maurice, Laurent Essioux, Philippe Millasseau, Pascale Grel, Virginie Debailleul, Anne-Marie Simon, Dominique Caterina, Isabelle Dufaure, Kattayoun Malekzadeh, Maria Belova, Jian-Jian Luan, Michel Bouillot, Jean-Luc Sambucy, Gwenael Primas, Martial Saumier, Nadia Boubkiri, Sandrine Martin-Saumier, Myriam Nasroune, Hélène Peixoto, Arnaud Delaye, Virginie Pinchot, Mariam Bastucci, Sophie Guillou, Magali Chevillon, Ricardo Sainz-Fuertes, Said Meguenni, Joan Aurich-Costa, Dorra Cherif, Anne Gimalac, Cornelia Van Duijn, Denis Gauvreau, Gail Ouelette, Isabel Fortier, John Realson, Tatiana Sherbatich, Nadejda Riazanskaia, Evgeny Rogaev, Peter Raeymaekers, Jeroen Aerssens, Frank Konings, Walter Luyten, Fabio Macciardi, Pak C. Sham, Richard E. Straub, Daniel R. Weinberger, Nadine Cohen, and Daniel Cohen, which appeared in number 21, October 15, 2002, of *Proc. Natl. Acad. Sci. USA* (**99,** 13675–13680; First Published October 3, 2002; 10.1073/pnas.182412499), the author name Gail Ouelette should have appeared as Gail Ouellette and the author name John Realson should have appeared as John Raelson. The corrected author line appears below. The online version has been corrected.

Ilya Chumakov, Marta Blumenfeld, Oxana Guerassimenko, Laurent Cavarec, Marta Palicio, Hadi Abderrahim, Lydie Bougueleret, Caroline Barry, Hiroaki Tanaka, Philippe La Rosa, Anne Puech, Nadia Tahri, Annick Cohen-Akenine, Sylvain Delabrosse, Sébastien Lissarrague, Françoise-Pascaline Picard, Karelle Maurice, Laurent Essioux, Philippe Millasseau, Pascale Grel, Virginie Debailleul, Anne-Marie Simon, Dominique Caterina, Isabelle Dufaure, Kattayoun Malekzadeh, Maria Belova, Jian-Jian Luan, Michel Bouillot, Jean-Luc Sambucy, Gwenael Primas, Martial Saumier, Nadia Boubkiri, Sandrine Martin-Saumier, Myriam Nasroune, Hélène Peixoto, Arnaud Delaye, Virginie Pinchot, Mariam Bastucci, Sophie Guillou, Magali Chevillon, Ricardo Sainz-Fuertes, Said Meguenni, Joan Aurich-Costa, Dorra Cherif, Anne Gimalac, Cornelia Van Duijn, Denis Gauvreau, Gail Ouellette, Isabel Fortier, John Raelson, Tatiana Sherbatich, Nadejda Riazanskaia, Evgeny Rogaev, Peter Raeymaekers, Jeroen Aerssens, Frank Konings, Walter Luyten, Fabio Macciardi, Pak C. Sham, Richard E. Straub, Daniel R. Weinberger, Nadine Cohen, and Daniel Cohen

www.pnas.org/cgi/doi/10.1073/pnas.262645899

IMMUNOLOGY. For the article "Negative autoregulation of BCL-6 is bypassed by genetic alterations in diffuse large B cell lymphomas," by Xing Wang, Zhiping Li, Akira Naganuma, and B. Hilda Ye, which appeared in number 23, November 12, 2002, of *Proc. Natl. Acad. Sci. USA* (**99,** 15018–15023; First Published October 29, 2002; 10.1073/pnas.232581199), the left axis label of Fig. 6 appeared incorrectly due to a printer's error. The corrected figure and its legend appear below.

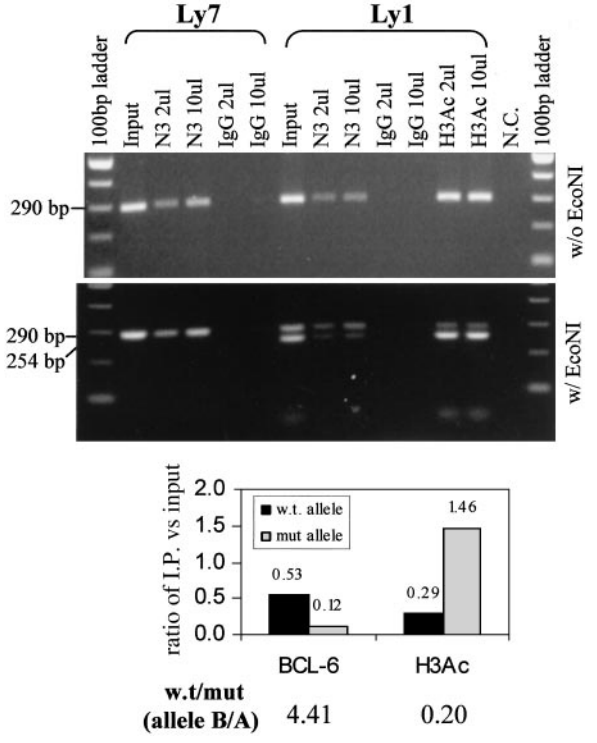

Fig. 6. BCL-6 preferentially binds to the wild-type exon 1 in Ly1 cells. Both Ly1 and the control Ly7 cells were analyzed for association of BCL-6 and acetylated H3 with the exon 1 sequence. Location of the PCR primers is given with respect to exon 1 and the surrounding mutations. Various amounts of recovered genomic DNA as well as a fraction of the total chromatin input were used in PCR reactions with the BCL-6-e1 and BCL-6 i2 primer pairs. IgG, normal rabbit IgG used as control antibody; N3, polyclonal anti-BCL-6 antibody; N.C., negative control PCR reaction with no template.

www.pnas.org/cgi/doi/10.1073/pnas.0136862100

COMMENTARY. For the article "The inner inner core of Earth," by Don L. Anderson, which appeared in number 22, October 29, 2002, of *Proc. Natl. Acad. Sci. USA* (**99,** 13966–13968; First Published October 21, 2002; 10.1073/pnas.232565899), the legend to Fig. 1 should have included the following statement. "Figure courtesy of M. Ishii."

www.pnas.org/cgi/doi/10.1073/pnas.0136631100